LPSC 2017 #2836

BASALTIC LITHIC CLASTS IN TYPE 1A AND 2A MESOSIDERITES: TREND TOWARDS A EUCRITIC COMPOSITION

Bastian Baecker[1] (bastian.baecker@nasa.gov), Barbara A. Cohen[1,2], Alan E. Rubin[3], Barbara Frasl[4] and Catherine M. Corrigan[5]

1 – NPP USRA / Planetary NSSTC, NASA Marshall S.F.C., 2 – Planetary, NASA Goddard S.F.C., 3 – IGPP & EPSS, UCLA, 4 – The University of Alabama in Huntsville (UAH), 5 – NMNH, Smithsonian Institution

1) MESOSIDERITE (MES) MYSTERY:

- ○ Enigmatic stony-iron meteorites & fragmental matrix breccias with irregular textures [1,2].
- ○ Roughly equal volumes of metal (Fe-Ni) and silicates -> strongly mixed.
- ○ Silicates: consist of basaltic, gabbroic, and pyroxenitic components = ± Eucrites/Howardites [3-8].
- ○ Silicates = strongly metamorphosed after formation = difficult to assess their origin.
  - ➡ Hence, tough assessment of MES parent body differentiation process [9,10].
- ○ MES silicates = **LIKELY** an origin and residence at the surface of a differentiated body [11],
- ○ **BUT!** Slow cooling rate of the metal points to an origin in the deep interior [12].

Possible EXPLANATIONS?

- ✓ **1st**: Large impacts and re-assembly of multiple precursors with differentiated or primitive origin - as the main cause for silicate/metal-mixing [e.g. 1,2].
- ✓ **2nd**: Mixing of near-surface silicates with the interior core-metal on a single parent body, caused by an event such as a catastrophic breakup [e.g. 11].
- ○ FOLLOWED BY: a) 2nd mixing events b) surface brecciation c) deep burial + slow cooling d) re-melting / metamorphosis

CENTRAL MOTIVATION:

- ○ Metallographic cooling rates on MES (~0.05 - 0.2 K/Ma) = **SLOW! HOWEVER** rapid nature of impact or breakup events; e.g. [10,13-15].
- ○ Do the exposure and thermal history result from cooling on their original parent body, the MES mixing event, or later impacts?

MAIN GOAL IN THIS PART (overall goals see [16]):

- ➢ 1st: Assess differences between lithic clasts of different MES as well as single grains by using petrography and electron microprobe elemental data.
- ➢ 2nd: Compare MES with groups of differentiated meteorites similar in mineralogy, texture and possible formation history; i.e. HEDs, anomalous and silicate bearing iron meteorites e.g. [4,7].

3) SEM RESULTS ON SELECTED MES LITHIC CLASTS, SINGLE GRAINS, AND METAL (px = pyroxene, plag = plagioclase, si = silica, phos = phosphate, m = metal)

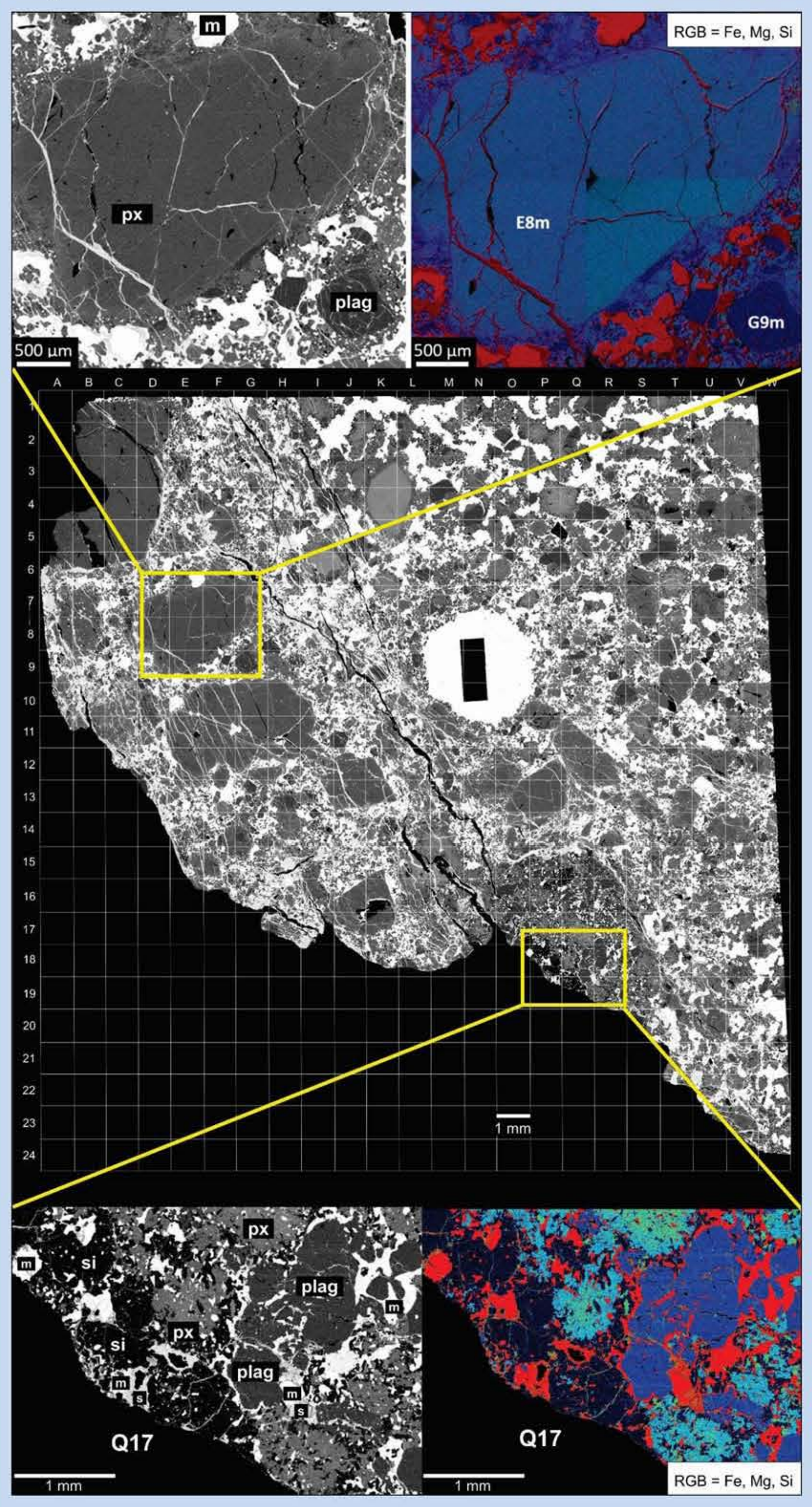

Fig.1. BSE / EDX images of **Mount Padbury** - ASU 927 (2A).

Lithic clast **Q17** (7.0 x 6.0 mm):
- ➢ Px, plag, silica, metal and sulfides.
- ➢ Some areas are fine-grained (50-200 µm).
- ➢ Clasts are partly rimmed by troilite (thickness ~100 µm).

Individual grain **E8m** (4.2 x 2.1 mm):
- large low-Ca px grain surrounded by Fe-Ni metal and adjacent to a plag grain (G9m).
- All grains show multiple cracks, many of which are filled with troilite.
- Many px grains exhibit BSE bright rims.

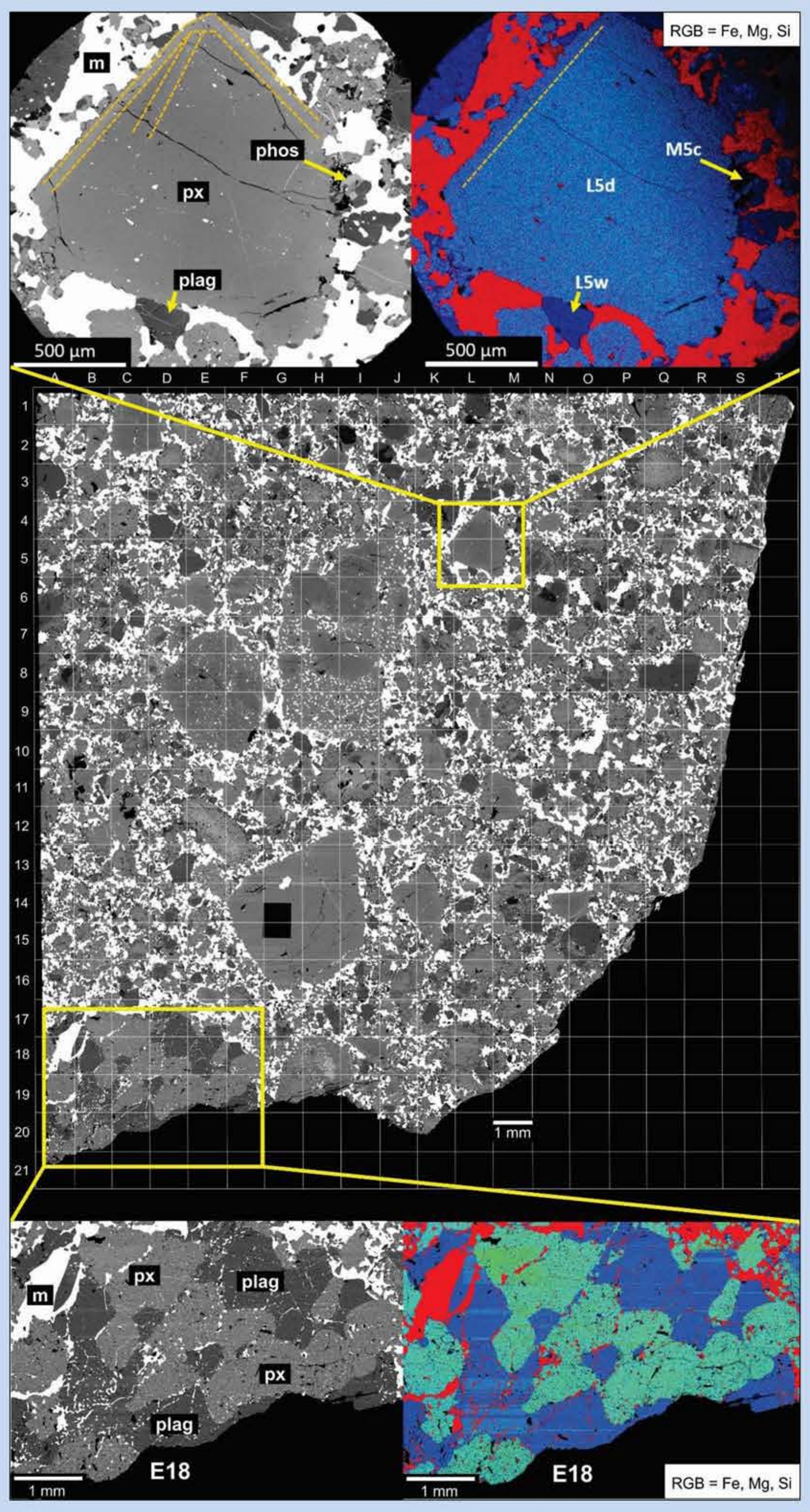

Fig.2. BSE / EDX images of **Clover Springs** - ASU 646.1 (2A).

Lithic clast **E18** (6.0 x 3.0 mm):
- ➢ Mainly px, plag and metal.
- ➢ Px- and plag form ~120° triple junctions
- ➢ Troilite (FeS) forms strings along px and plag boundaries.
- ➢ In few cases, strings occur inside px and plag, probably along exsolution lamellae.

Individual grain **L5d** (1.7 x 1.5 mm):
- large low-Ca px grain with BSE bright rim.
- Surrounded by Fe-Ni metal, merrillite (M5c) and plag (L5w).
- Grains show multiple fractures + voids, filled with Fe-Ni metal, sulfides and oxides.

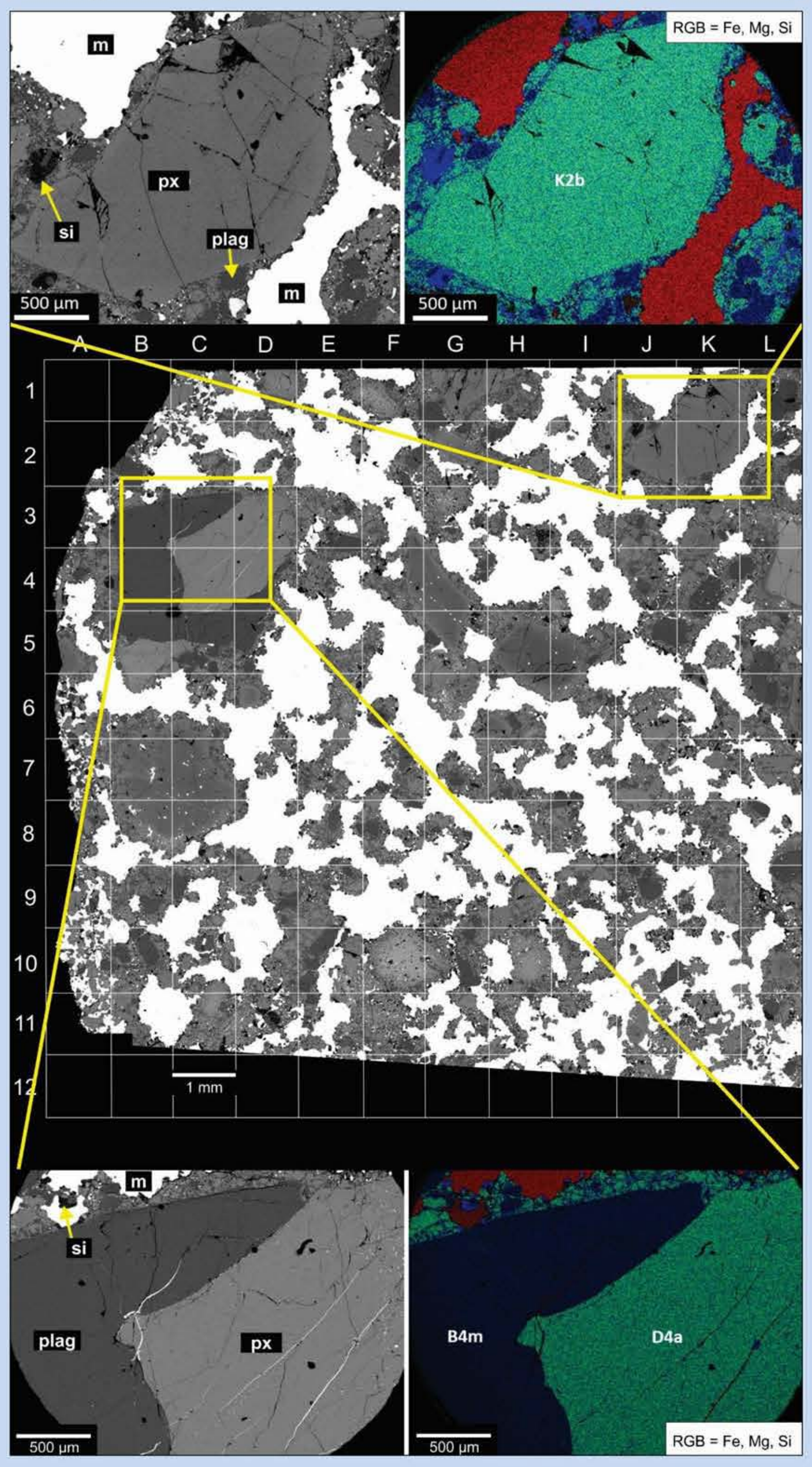

Fig.3. BSE / EDX images of **Patwar** - ASU 634-1-4 (1A).

(possible) Lithic clast **C4** (3.2 x 2.5 mm):
- ➢ Composed of two anhedral plag (B4m) and low-Ca px grains (D4a) surrounded by troilite.
- ➢ The low-Ca px contains abundant exsolution lamellae. Inside the clast troilite blebs and multiple cracks filled with troilite are observable.

Individual grain **K2b** (2.5 x 1.5 mm):
- Large low-Ca px grain rimmed by troilite.
- Exhibits multiple cracks, none of which are filled with troilite.

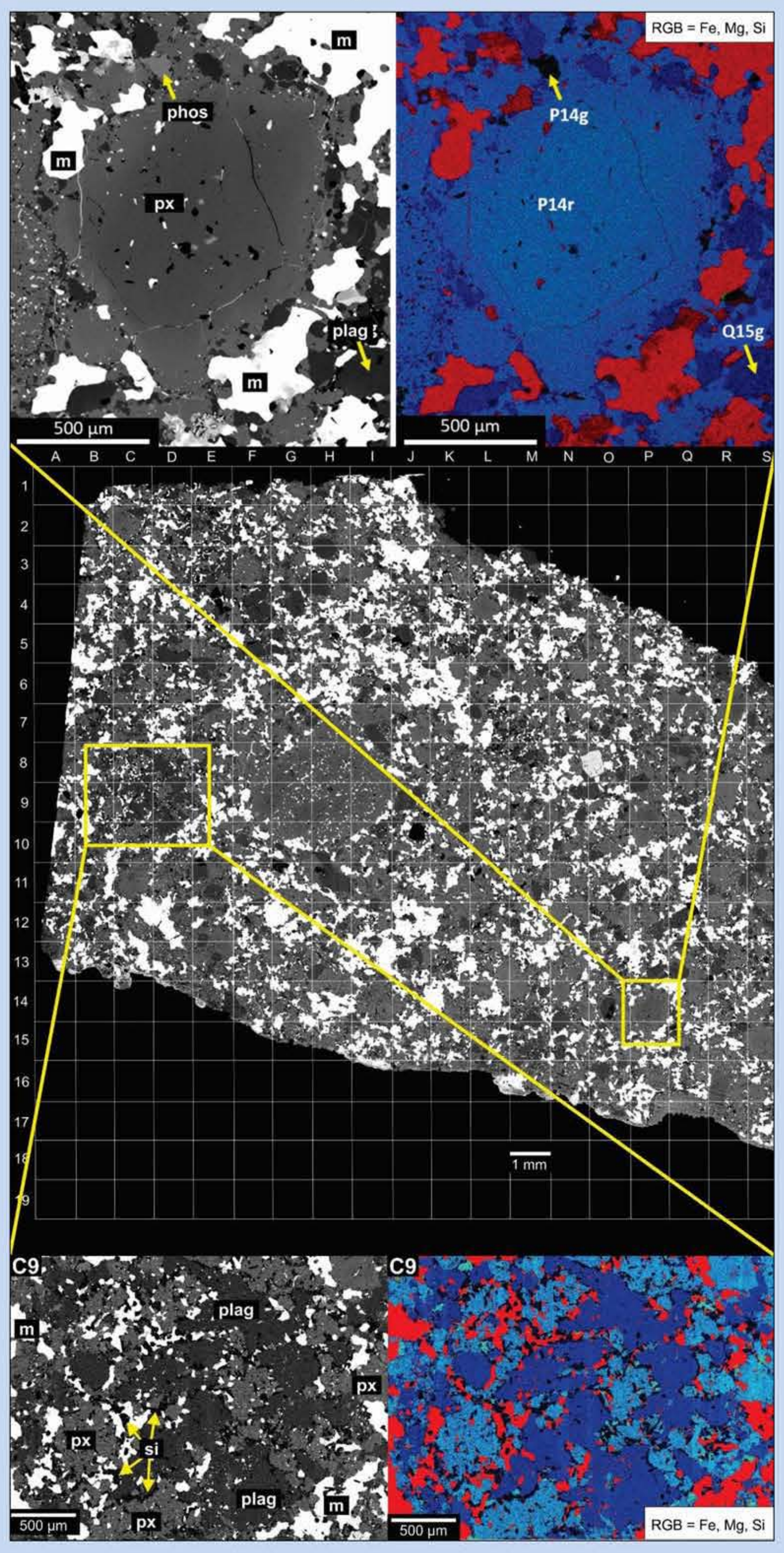

Fig.4. BSE / EDX images of **NWA 1242** (1A).

Lithic clast **C9** (3.0 x 2.5 mm):
- ➢ Px, plag, silica and metal.
- ➢ Crystals of silica and metal partly envelope px and plag and partly interstitial between them (RGB image).

Individual grain **P14r** (1.2 x 1.0 mm):
- Low-Ca px grain close to Fe-Ni metal, merrillite and plag.
- Grains separated by µm-sized aggregates of px.
- Subangular & porous.
- Multiple cracks filled with troilite.
- BSE bright rim.

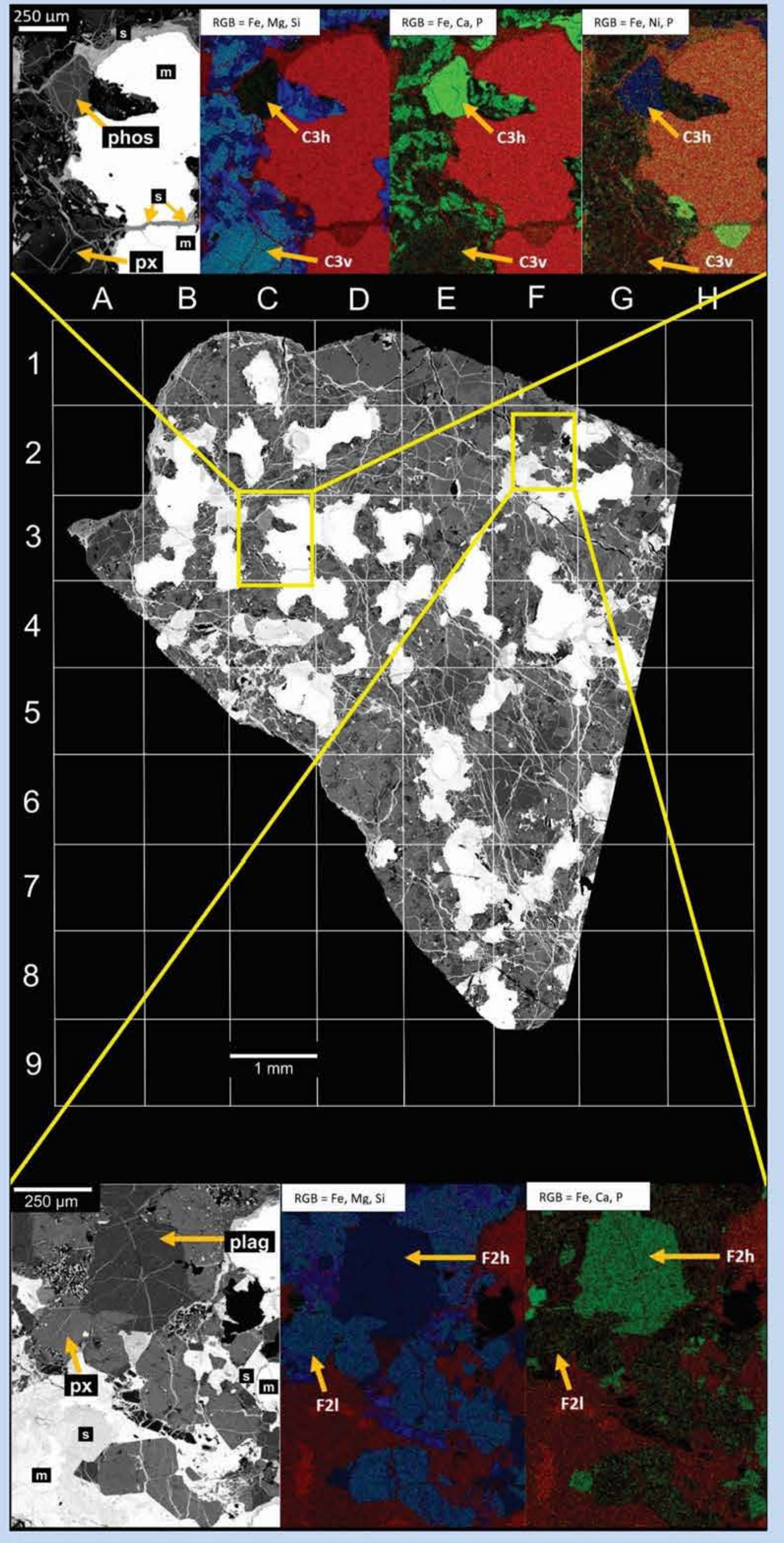

Fig.5. BSE / EDX images of **Toufassour.** A weathered MES exhibiting many limonite veins.

(possible) Lithic clast **F2** (1.2 x 1.0 mm):
- ➢ Assemblage of low-Ca px and plag.
- ➢ Fine-grained and granular along with angular grains indicating metamorphism and annealing.
- ➢ Cracks filled with troilite.

Individual grains **C3v -** 500 x 350 µm; **C3h** - 220 x 200 µm:
- C3v (low-Ca px) and C3h (merrillite).
- In proximity to large Fe-Ni grains (1-5 mm).
- Grains exhibit cracks filled with troilite.

4) ELECTRON MICROPROBE RESULTS & DISCUSSION:

- ☐ Similarities and differences => silicates MES + HEDs.
- ☐ MES lithic clasts resemble eucrites in their modal abundances [17].
- ☐ **Fig. 5A**:
  - ❖ The single-grain px are more Mg-rich than typical eucrites - closer in composition to the low Ca-px in diogenites. This could be indicative for single grains derived from more fragile (more breakable) diogenetic lithologies whereas lithic clasts derive from a more eucritic origin.
  - ❖ Low-Ca px in lithic clasts trend toward more Fe-rich compositions typical of eucrites and eucritic Vaca Muerta pebbles. Some results measured for MES (e.g. Dyarrl Island (1A) and Morristown (3A)) from other studies show a similar trend [18].
  - ❖ Low-Ca px in Patwar and (partly Clover Springs) measured for both single grains and lithic clasts have a more eucritic composition.
- ☐ This similarity is also observable in **Fig. 5B**.
  - ❖ Overall, most single grains seem to plot close to the Stannern trend indicative of partial melting [19].
  - ❖ Lithic clasts of Clover Springs and Patwar plot on the the Nuevo Laredo trend reflecting fractional crystallization [6] (as also found for eucritic Vaca Muerta pebbles [20]).
  - ❖ However, most other lithic clasts (60%) plot closer to the single grain composition.
- ☐ Overall, there is a visible, distinct shift between the groups of single grains and lithic clasts which might be indicative for a different mineralogical origin and history.
- ☐ We can infer that minerals and metals in lithic clasts should have a common (thermal) history.

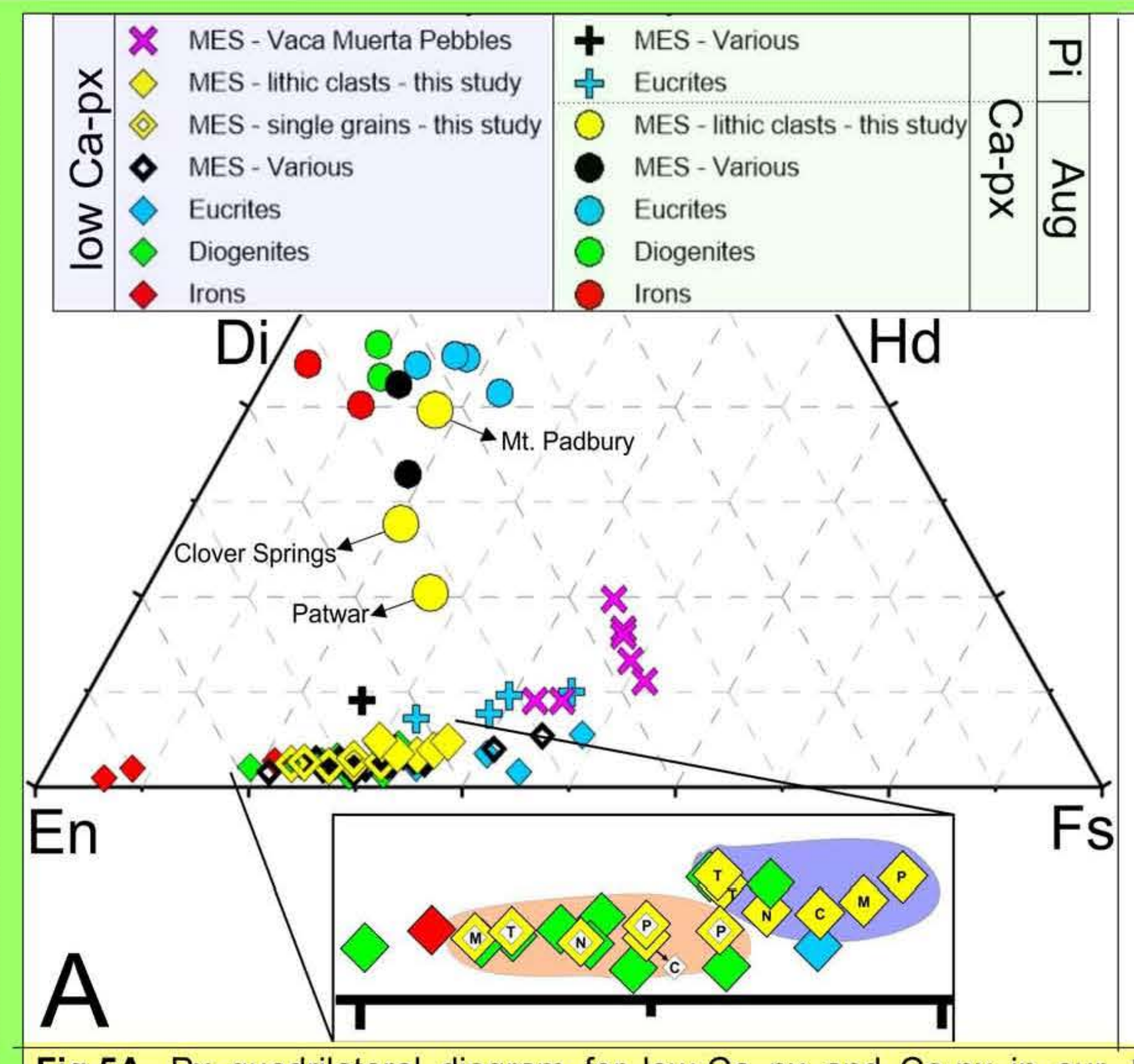

Fig.5A. Px quadrilateral diagram for low-Ca px and Ca-px in our data, various MES, eucrites, diogenites and iron meteorites. We measured multiple points for lithic clasts and single grains in each MES silicate. Plotted are the average mean of the points for each MES, respectively. Additional MES data were adapted from [17], [18], [21-23]. Vaca Muerta Pebble data is from [24]; eucrite and diogenite data from [25] and iron meteorite data from [26, 27].

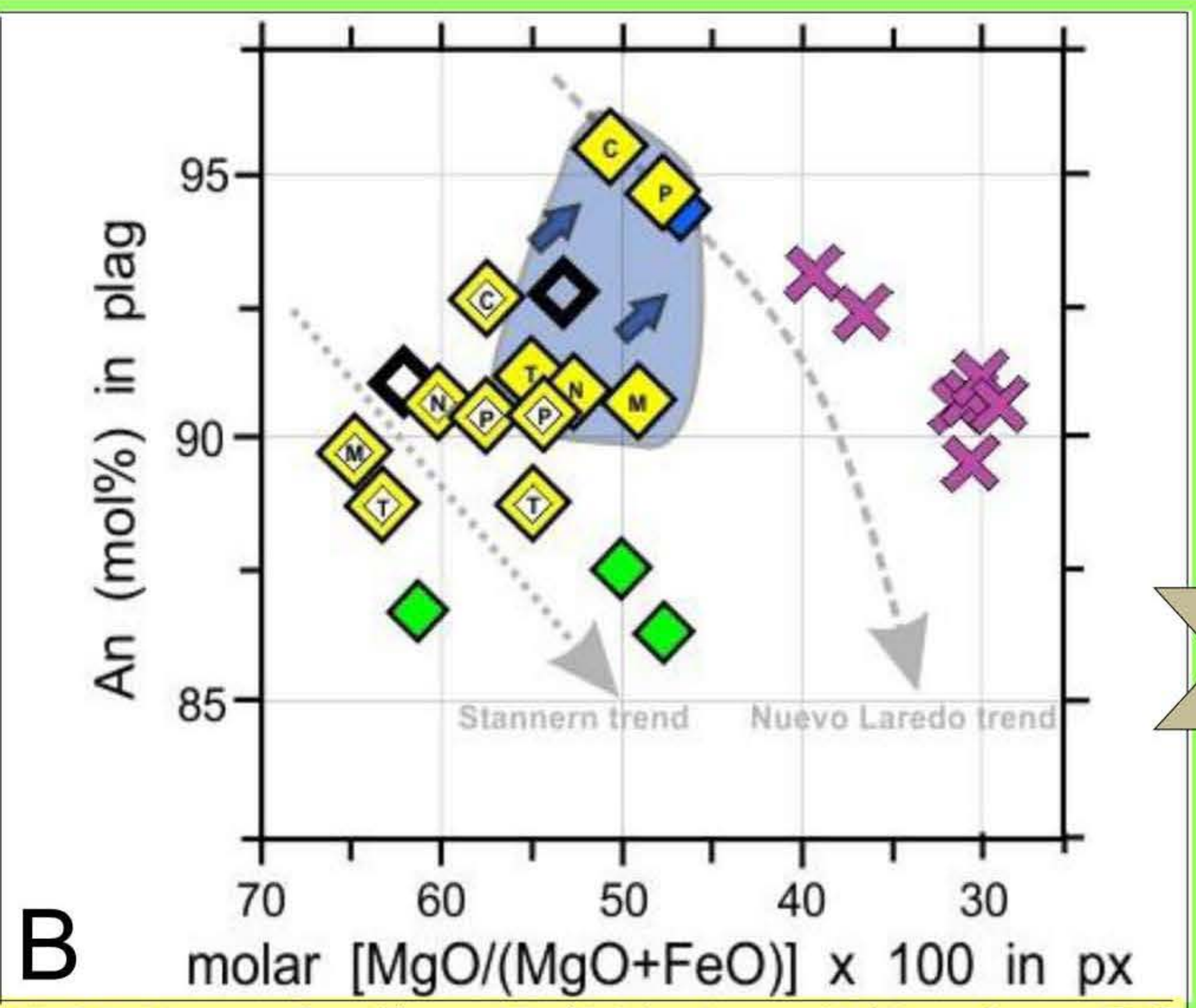

Fig.5B. Diagram of mol% anorthite (An) in plag vs. Mg* in px for our MES data. Eucrite trends from [19]; MES data from [22, 24, 25]. Two lithic clasts - Patwar (**P**), Clover Springs (**C**) - plot on the Nuevo Laredo trend (fractional crystallization). Lithic clasts of NWA 1242 (**N**), Toufassour (**T**) and Mt. Padbury (**M**) seem to be shifted towards the eucritic composition of the Vaca Muerta pebbles. Individual mineral grains of Mt. Padbury, Patwar, Clover Springs, Toufassour and NWA 1242 plot closer to the Stannern trend (partial melting).

5) FUTURE WORK:

- ➢ Analyze the noble-gas complement (He-Xe) of the lithic clasts and single grains. Assess Ar-Ar and cosmic-ray exposure ages using the MSFC state-of-the-art Noblesse (Nu Instruments, UK) MS = new high sensitivity + multi-ion-detection.
- ➢ Measure the metallographic cooling rates and compare them to Ar-Ar ages for each clast; if these agree within single clasts, we can infer closure temperatures connected to the burial depth.
- ➢ Measuring oxygen isotopes for selected lithic clasts.
- ➢ If material allows, we will then measure Sm, Yb and Eu in the clasts to compare with HEDs.

References: [1] Powell B. N. (1971) GCA, 35:5-34. [2] Floran R. J. (1978) Proc. Lunar Planet. Sci. Conf. 9th, 1053-1081. [3] McCall G. J. H. (1966) Mineral. Mag.,35:1029-1060. [4] Mittlefehldt D. W. et al. (1979) GCA, 43:673-688. [5] Ikeda Y. et al. (1990) Ant. Met. Res., 3:99. [6] Kimura M. et al. (1991) Ant. Met. Res., 4:263. [7] Rubin A. E. and Mittlefehldt D. W. (1992) GCA, 56:827-840. [8] Mittlefehldt D. W. (2014) 77th Ann. Met. Soc. Meeting (Abs. #5313). [9] Crozaz G. and Tasker D. R. (1981) GCA, 45:2037-2046. [10] Keil K. et al. (1994) Plan. Space Sci., 42:1109-1122. [11] Delaney J. S. (1983) Meteoritics, 18:289-290. [12] Bogard D. D. et al.(1990) GCA, 54:2549-2564. [13] Wasson J. T. and Hoppe P. (2014) 77th Ann. Met. Soc. Meeting (Abs. #5405). [14] Hopfe W. D. and Goldstein J. I. (2001) MAPS, 36:135-154. [15] Goldstein J. I. et al. (2009) Chemie der Erde-Geochem., 69:293-325. [16] Baecker B. and Cohen B. A. (2016) 47th LPSC (Abs. #2179). [17] Prinz M. et al. (1980) Lunar Planet. Sci., 11:1055-1071. [18] Mason B. and Jarosewich E. (1973). Miner. Mag, 39:204-215. [19] Buchanan P. C. and Reid A. M. (1991) Lunar Planet Sci., 22:149-150. [20] Rubin A. E. and Mittlefehldt D. W. (1992) GCA, 56:827-840. [21] Agosto W. N et al. (1980) Lunar Planet. Sci., 11:1027-1045. [22] Terribilini D. et al. (2000). MAPS, 35:617-628. [23] Prinz M. et al. (1982) Lunar Planet. Sci., 13:631. [24] Rubin A. E. and Jerde E. A. (1987) EPSL, 84:1-14. [25] Mittlefehldt D. W. et al. (1998) Planet. Mater. Rev. Mineral. Geochem. 36, 4.1-4.195. [26] Olsen E. J. et al. (1996) Science, 273:1365. [27] Ruzicka A. and Hutson M. (2010) GCA, 74:394-433.

Acknowledgement: We thank the ASU Center for Meteorite Studies and NASA JSC for MES specimens. We thank Rosario Esposito for technical assistance with the UCLA e-probe. This work was supported by the NASA/USRA postdoctoral program.